



**HAL**  
open science

## The influence of temperature (up to 120 °C) on the thermal conductivity of variably porous andesite

Michael Heap, Gunel Alizada, David Jessop, Ben Kennedy, Fabian Wadsworth

### ► To cite this version:

Michael Heap, Gunel Alizada, David Jessop, Ben Kennedy, Fabian Wadsworth. The influence of temperature (up to 120 °C) on the thermal conductivity of variably porous andesite. *Journal of Volcanology and Geothermal Research*, 2024, pp.108140. 10.1016/j.jvolgeores.2024.108140 . hal-04655074

**HAL Id: hal-04655074**

**<https://hal.science/hal-04655074>**

Submitted on 26 Jul 2024

**HAL** is a multi-disciplinary open access archive for the deposit and dissemination of scientific research documents, whether they are published or not. The documents may come from teaching and research institutions in France or abroad, or from public or private research centers.

L'archive ouverte pluridisciplinaire **HAL**, est destinée au dépôt et à la diffusion de documents scientifiques de niveau recherche, publiés ou non, émanant des établissements d'enseignement et de recherche français ou étrangers, des laboratoires publics ou privés.



Distributed under a Creative Commons Attribution 4.0 International License



## The influence of temperature (up to 120 °C) on the thermal conductivity of variably porous andesite

Michael J. Heap<sup>a,b,\*</sup>, Gunel Alizada<sup>a,c</sup>, David E. Jessop<sup>d,e</sup>, Ben M. Kennedy<sup>f</sup>, Fabian B. Wadsworth<sup>g</sup>

<sup>a</sup> Université de Strasbourg, CNRS, Institut Terre et Environnement de Strasbourg, UMR 7063, 5 rue Descartes, Strasbourg F-67084, France

<sup>b</sup> Institut Universitaire de France (IUF), Paris, France

<sup>c</sup> UNISTRA, Azerbaijan State Oil and Industry University, French Azerbaijani University, 183 Nizami Street, Baku, Azerbaijan

<sup>d</sup> CNRS, IRD, OPGC Laboratoire Magmas et Volcans, Université Clermont Auvergne, F-63000 Clermont-Ferrand, France

<sup>e</sup> Université de Paris, Institut de Physique du Globe de Paris, CNRS UMR 7154, F-75005 Paris, France

<sup>f</sup> Department of Geological Sciences, University of Canterbury, Private Bag 4800, Christchurch, New Zealand

<sup>g</sup> Department of Earth Sciences, Durham University, Durham DH1 3LE, UK

### ARTICLE INFO

#### Keywords:

Thermal conductivity  
Temperature  
Volcano  
Geothermal reservoir  
Hot disk  
Andesite  
Thermal modelling

### ABSTRACT

The thermal conductivity of volcanic rock is an essential input parameter in a wide range of models designed to better understand volcanic and geothermal processes. However, although volcanoes and geothermal reservoirs are often characterised by temperatures above ambient, laboratory thermal conductivity measurements are often performed at ambient temperature. In addition, there are currently few data on the temperature dependence of thermal conductivity for andesite, a common volcanic rock. Here, we provide elevated-temperature (up to 120 °C) laboratory measurements of thermal conductivity for variably porous (~0.05 to ~0.6) and variably glassy andesites from Mt. Ruapehu (New Zealand) using the transient hot-strip method. Our data show that (1) the thermal conductivity of these andesites has little to no temperature dependence and, therefore, (2) there is also no influence of porosity on the temperature dependence of thermal conductivity. We compare our new data with compiled published data to show that the thermal conductivity of volcanic rocks may decrease, remain constant, or increase as a function of temperature. We show that the thermal conductivity of amorphous glass and crystalline material increase and decrease, respectively, as temperature increases. We therefore interpret the temperature dependence of the thermal conductivity of volcanic rock to be dependent on glass content. The thermal conductivity of the studied andesites, the microstructure of which can be characterised by phenocrysts within a variably glassy groundmass, has little to no temperature dependence because the decrease in the thermal conductivity of the crystalline materials, due to decreases in lattice thermal conductivity, is offset by the increase in the thermal conductivity of the amorphous glass. A simple modelling approach, using the temperature dependence of the thermal conductivity of glass and crystalline material, provides a crystal content of 0.26 for a thermal conductivity independent of temperature, a common crystal content for andesite dome rock. Our findings imply that calculations of heat transfer through partially glassy volcanic rocks need not consider a temperature-dependent thermal conductivity, but that decreases and increases in thermal conductivity with temperature should be expected for fully crystallised or devitrified volcanic rocks and completely glassy volcanic rocks, respectively. We highlight that more experimental studies are now required to assess the evolution of thermal conductivity as a function of temperature in a wide range of volcanic rocks with different crystallinities.

### 1. Introduction

The thermal properties of volcanic rocks are important input

parameters in a wide range of models designed to understand heat transfer in active volcanoes and igneous systems (Irvine, 1970; Norton and Knight, 1977; Huppert and Sparks, 1981; Carrigan, 1984; Bruce and

\* Corresponding author at: Université de Strasbourg, CNRS, Institut Terre et Environnement de Strasbourg, UMR 7063, 5 rue Descartes, Strasbourg F-67084, France.

E-mail address: [heap@unistra.fr](mailto:heap@unistra.fr) (M.J. Heap).

<https://doi.org/10.1016/j.jvolgeores.2024.108140>

Received 15 December 2023; Received in revised form 9 July 2024; Accepted 9 July 2024

Available online 11 July 2024

0377-0273/© 2024 The Authors. Published by Elsevier B.V. This is an open access article under the CC BY license (<http://creativecommons.org/licenses/by/4.0/>).

Huppert, 1989; Carrigan et al., 1992; Fialko and Rubin, 1999; Wooster et al., 1997; Annen et al., 2008; Nabelek et al., 2012; Annen, 2017; Tsang et al., 2019; Loncar and Huppert, 2022; Klein et al., 2024) and in geothermal reservoirs (Canet et al., 2015; Gunnarsson and Aradóttir, 2015; Carlino et al., 2016; Wadsworth et al., 2017; Vélez et al., 2018; González et al., 2022; Burchardt et al., 2022). The thermal properties of volcanic rocks are also important to assess their potential as heat storage materials (Nahhas et al., 2019; Liu et al., 2020).

In terms of volcanic and igneous processes, Annen (2017) used values of thermal conductivity, thermal diffusivity, and specific heat capacity in mathematical models designed to understand the thickness of thermal aureoles surrounding intrusions. Values of thermal conductivity, thermal diffusivity, and specific heat capacity were also used by Loncar and Huppert (2022) in mathematical models designed to better understand the shape changes and cooling regimes of dykes upon intrusion. Klein et al. (2024) used thermal conductivity values from Heap et al. (2022) to calculate heat flux during an ongoing unrest phase of La Soufrière de Guadeloupe (Eastern Caribbean), and also to infer the permeability of the edifice. The importance of understanding the heat flux of a volcano is underscored by the link between an increase in the heat flux of a volcano and an eruption (Girona et al., 2021). In terms of geothermal energy exploration and exploitation, Vélez et al. (2018) measured the thermal conductivity of rocks collected from Nevada del Ruiz volcano (Colombia) to be used in numerical modelling designed to simulate the distribution of temperature in the reservoir and, therefore, to estimate its geothermal potential. Burchardt et al. (2022) used values of thermal conductivity and specific heat capacity in finite element models designed to assess the influence of different combinations of dyke and sill thickness and number on the geothermal potential of typical Icelandic calderas.

In all these modelling studies, and others, values of thermal conductivity for the volcanic unit or units within the model are often taken to be constant, and are often taken from laboratory investigations in which thermal conductivity was measured at ambient temperature. However, the temperature within volcanoes and geothermal reservoirs is often above ambient, and experimental studies have shown that the thermal conductivity of rock is typically reduced as temperature is increased (see compilations in Desai et al., 1974; Čermák and Rybach, 1982; Clauser and Huenges, 1995; Vosteen and Schellschmidt, 2003; Merriman et al., 2018; Norden et al., 2020; Clauser, 2021).

The majority of experimental studies that provide laboratory thermal property data at elevated temperatures have done so for granitic and sedimentary rocks (Desai et al., 1974; Čermák and Rybach, 1982; Clauser and Huenges, 1995; Vosteen and Schellschmidt, 2003; Norden et al., 2020; Clauser, 2021). Numerous laboratory studies have shown that the thermal conductivity of granitic rocks decreases as a function of temperature (Pribnow et al., 1996; Seipold, 1998; Vosteen and Schellschmidt, 2003; Mottaghy et al., 2008; Miao et al., 2014; Merriman et al., 2018; Miranda et al., 2019; Norden et al., 2020). For example, the thermal conductivity of granite from the North China Craton (China) was reduced from  $\sim 1.25 \text{ W}\cdot\text{m}^{-1}\cdot\text{K}^{-1}$  at room temperature to  $\sim 0.5 \text{ W}\cdot\text{m}^{-1}\cdot\text{K}^{-1}$  at a temperature of  $900 \text{ }^\circ\text{C}$  (Miao et al., 2014). Laboratory studies have also shown that the thermal conductivity of sedimentary rocks decreases as a function of temperature (Clauser and Huenges, 1995; Vosteen and Schellschmidt, 2003; Abdulagatova et al., 2009; Merriman et al., 2018; Norden et al., 2020; Chen et al., 2021; Emirov et al., 2021). For example, Vosteen and Schellschmidt (2003) showed that the mean thermal conductivity of a collection of sandstones and carbonate rocks was reduced from  $\sim 3.0 \text{ W}\cdot\text{m}^{-1}\cdot\text{K}^{-1}$  at room temperature to  $\sim 1.5 \text{ W}\cdot\text{m}^{-1}\cdot\text{K}^{-1}$  at a temperature of  $300 \text{ }^\circ\text{C}$ . Clauser and Huenges (1995) also found that an increase in temperature systematically decreased the thermal conductivity of clastic and carbonate rocks, from  $\sim 3.0 \text{ W}\cdot\text{m}^{-1}\cdot\text{K}^{-1}$  at room temperature to  $\sim 1.0 \text{ W}\cdot\text{m}^{-1}\cdot\text{K}^{-1}$  at  $800 \text{ }^\circ\text{C}$ . Using the laser flash analysis (LFA) method, Merriman et al. (2018) showed that the thermal conductivity of calcite, and a number of carbonate rocks (limestone, dolomite, marble), decreases as a function of

temperature (up to  $\sim 625 \text{ }^\circ\text{C}$ ). For example, in their dataset, the thermal conductivity of Carrara marble decreased from  $\sim 1.8 \text{ W}\cdot\text{m}^{-1}\cdot\text{K}^{-1}$  at room temperature to  $\sim 1.0 \text{ W}\cdot\text{m}^{-1}\cdot\text{K}^{-1}$  at  $425 \text{ }^\circ\text{C}$ .

Although the number of studies that aim to better understand the thermal properties of volcanic rocks has increased over the last years (Horai et al., 1970; Fujii and Osako, 1973; Robertson and Peck, 1974; Bagdassarov and Dingwell, 1994; Whittington et al., 2009; Romine et al., 2012; Lenhardt and Götz, 2015; Mielke et al., 2015; Hofmeister et al., 2016; Mielke et al., 2016, 2017; Balkan et al., 2017; Vélez et al., 2018; Heap et al., 2020; Hofmeister, 2020; Weydt et al., 2021; Heap et al., 2022), fewer studies provide data on the temperature dependence of thermal conductivity for volcanic rocks. The compiled data in Desai et al. (1974) and Čermák and Rybach (1982), reviewed in Clauser and Huenges (1995), show that (1) the thermal conductivity of tuff and some basalts decreases as a function of temperature, (2) the thermal conductivity of some basalts and some diabases does not appreciably or systematically change as a function of temperature, and (3) that the thermal conductivity of basaltic glass, diabase glass, and obsidian increases as a function of temperature. For example, the thermal conductivity of basalt from Kyushu (Japan) decreased from 2.37 to  $1.34 \text{ W}\cdot\text{m}^{-1}\cdot\text{K}^{-1}$  as temperature was increased from 0 to  $700 \text{ }^\circ\text{C}$  (Kawada, 1964), and the thermal conductivity of obsidian from Newberry caldera (Oregon, USA) increased from  $1.26 \text{ W}\cdot\text{m}^{-1}\cdot\text{K}^{-1}$  at room temperature to  $4.13 \text{ W}\cdot\text{m}^{-1}\cdot\text{K}^{-1}$  at a temperature of  $\sim 1400 \text{ }^\circ\text{C}$  (Murase and McBirney, 1970). Using the LFA method, Romine et al. (2012) showed that the thermal conductivity of rhyolite glass increased from  $\sim 1.15 \text{ W}\cdot\text{m}^{-1}\cdot\text{K}^{-1}$  at room temperature to  $1.5 \text{ W}\cdot\text{m}^{-1}\cdot\text{K}^{-1}$  at a temperature of  $\sim 1225 \text{ }^\circ\text{C}$ . Chen et al. (2021) found that the thermal conductivity of felsite and spilite decreased as a function of temperature, but that the thermal conductivity of perlite, andesite-basalt, and pitchstone increased up to a temperature of  $\sim 150 \text{ }^\circ\text{C}$  before decreasing up to the maximum temperature of  $300 \text{ }^\circ\text{C}$ . Mostafa et al. (2004) found that the thermal conductivity of four basalts from Egypt either did not appreciably change or decreased up to temperatures of  $\sim 625 \text{ }^\circ\text{C}$ , with the largest changes occurring above a temperature of  $\sim 300 \text{ }^\circ\text{C}$ . Nahhas et al. (2019) found that the thermal conductivity of two basalt samples did not appreciably or systematically change as temperature was increased up to  $700 \text{ }^\circ\text{C}$ . Using the LFA method, Hofmeister (2020) showed that the thermal conductivity of an andesite from Mt. Shasta (USA) did not change appreciably or systematically as temperature was increased up to almost  $900 \text{ }^\circ\text{C}$ . Finally, the thermal conductivity of a suite of  $>2$ -billion-year-old rhyolites from the Bundelkhand Craton (India) was found to decrease as a function of temperature, up to  $300 \text{ }^\circ\text{C}$  (Ray et al., 2023). The thermal conductivity of one rhyolite sample measured by Ray et al. (2023) decreased from  $\sim 3.3$  to  $\sim 2.4 \text{ W}\cdot\text{m}^{-1}\cdot\text{K}^{-1}$  as temperature was increased from  $\sim 30$  to  $\sim 300 \text{ }^\circ\text{C}$ .

Compared to granitic and sedimentary rocks, for which the thermal conductivity systematically decreases as a function of temperature (Desai et al., 1974; Čermák and Rybach, 1982; Clauser and Huenges, 1995; Vosteen and Schellschmidt, 2003; Merriman et al., 2018; Norden et al., 2020; Clauser, 2021), the influence of temperature on the thermal conductivity of volcanic rocks appears to be variable, and can increase, decrease, or remain constant. As a result, and despite the aforementioned laboratory studies, and others, our understanding of the thermal conductivity of volcanic rocks, and therefore our understanding of heat transfer in volcanoes and geothermal reservoirs, stands to benefit from new laboratory data. In particular, little is known on how porosity influences the temperature dependence of the thermal conductivity of volcanic rocks and there are very few data available for andesite, a very common volcanic rock. Here, therefore, we report findings from a laboratory study in which we measured the influence of temperature on the thermal conductivity of a suite of variably porous andesites.

## 2. Materials and methods

### 2.1. Experimental materials

A suite of variably-porous andesite samples, collected at Mt. Ruapehu (Taupō Volcanic Zone, New Zealand), were used for this study. This suite of andesites has been previously used in [Heap and Kennedy \(2016\)](#), who measured their permeability, and [Heap et al. \(2020\)](#), who measured their thermal properties at room temperature. The andesites are porphyritic and contain plagioclase and pyroxene phenocrysts hosted within a variably microlite-rich groundmass ([Fig. 1](#)). The samples with the lowest porosities ( $< 0.05$ ) are light grey in colour and their groundmasses appear more crystallised than the other samples (e.g., sample R3; [Fig. 1a](#)). The samples with higher porosity ( $> 0.1$ ) are dark grey in colour and have variably glassy groundmasses that contain microlites (e.g., samples R8, R10, R14, and R17; [Fig. 1c-f](#)). The andesites are variably porous and the increase in porosity is associated with an increase in the number and diameter of pores ([Fig. 1](#)). All of the andesites contain abundant microcracks ([Fig. 1](#)).

### 2.2. Experimental methods

Two cylindrical samples (20 mm in diameter and 40 mm in length) were prepared from each of the 17 blocks collected. These samples were washed and then dried in a vacuum-oven at 40 °C for at least 48 h. The connected porosity of each sample was calculated using the bulk sample volume and the skeletal (solid) sample volume measured by a helium pycnometer. The thermal conductivity,  $\lambda$  (in units of  $\text{W}\cdot\text{m}^{-1}\cdot\text{K}^{-1}$ ), of the samples was measured using a Hot Disk® TPS 500 Thermal Constants Analyser using the Transient Plane Source (TPS) method ([Gustafsson, 1991](#); [Harlé et al., 2019](#); [Heap et al., 2020, 2022](#)). The TPS method, a periodic method of thermal property measurement, uses a resistive sensor (the transient plane source) sandwiched between two samples to measure the increase in resistance as it heats the samples using an electrical current pulse. Because the geometry of the sensor is known, the average temperature increase as a function of time can be calculated, which can be then used to determine the thermal conductivity. The resistive sensor is therefore used as both the heat source and the temperature sensor. In our setup, the resistive sensor consists of two 10  $\mu\text{m}$ -thick nickel foil spirals (radius of 3.189 mm) that are encased and insulated by 30  $\mu\text{m}$ -thick Kapton (see inset in [Fig. 2a](#)). We used the “red cable” sensor supplied by Hot Disk®, which has a maximum working temperature of 180 °C. Measurements were made by sandwiching the sensor between two cylindrical samples cored from the same block ([Fig. 2a](#)). A good contact between the sensor and the surface of the samples was ensured by tightening a screw positioned at the top of the sample jig. To perform the measurements, the entire sample assembly was placed inside an electric box furnace with a maximum temperature of 200 °C ([Fig. 2b](#)). Measurements were made at room temperature (20–22 °C), 40, 60, 80, 100, and 120 °C. Although the maximum working temperature of the sensor and cable supplied by Hot Disk® is 180 °C, we chose a maximum temperature of 120 °C to (1) avoid any possibility of damaging the sensor and/or cable and (2) prevent the formation of thermal microcracks, which would influence our measurements. Although temperatures can reach 300–500 °C, temperatures up to 120 °C are also of interest for shallow hydrothermal systems at active volcanoes (e.g., [Chiodini et al., 2021](#); [Moune et al., 2022](#)) and volcanic geothermal reservoirs (e.g., [Arellano et al., 2003](#)). Once the sample assembly had equilibrated to the target temperature, an electrical current of known power and for a fixed duration was passed through the sensor, which then recorded the increase in sample temperature as a function of time. The output power and test duration used were 80–220 mW and 10 s, respectively. Four consecutive measurements were performed on each sample pair (on the four different combinations of sample end-faces), and we report herein the mean and standard deviation of the mean of these four measurements. For each

measurement, it is assumed that the thermal diffusivity remains constant over the period of measurement. Each measurement was performed at least 10–15 min apart to ensure that the samples and sample assembly had re-equilibrated to the target temperature. We used the Isotropic Hot Disk® Measurement Module for all measurements.

The standard uncertainty for values of thermal conductivity and thermal diffusivity using the transient hot-strip method has been determined to be 2.6 and 11%, respectively ([Hammerschmidt and Sabuga, 2000](#)). Measurement uncertainty using this technique arises from contact losses and ballistic radiative transfer gains ([Hofmeister, 2018](#)). We further note that contact losses would not be expected to change as a function of temperature. Similarly, ballistic radiative transfer gains would only be expected to increase with increasing temperature at reasonably high temperatures at which radiation dominates ([Hofmeister, 2018](#)); these high temperatures are far higher than the temperature range used here (note that the radiative power increases with  $T^4$ ; [Howell et al., 2023](#)). To provide an assessment of the precision of our Hot Disk® TPS 500 Thermal Constants Analyser, we measured the thermal conductivity of the same sandstone sample 100 times and found the standard error to be  $0.007 \text{ W}\cdot\text{m}^{-1}\cdot\text{K}^{-1}$  ([Heap et al., 2023](#)).

To help validate our setup and method, we first measured the thermal conductivity of Fontainebleau sandstone (100% quartz; [Bourbié and Zinsner, 1985](#)) and Indiana limestone (100% calcite; [Baud et al., 2021](#)) using same approach and conditions described above. For these samples, the output power and test duration used were 180–250 mW and 5–10 s, respectively. It is well known that the thermal conductivity of sandstone and limestone is systematically reduced as temperature is increased ([Clauser and Huenges, 1995](#); [Vosteen and Schellschmidt, 2003](#); [Abdulagatova et al., 2009](#); [Merriman et al., 2018](#); [Norden et al., 2020](#); [Chen et al., 2021](#); [Emirov et al., 2021](#)) and so, observing a similar trend would add confidence to our approach and to our new data collected for the andesites.

Our data show that the thermal conductivity of Fontainebleau sandstone and Indiana limestone indeed decreased systematically as a function of temperature ([Fig. 3a](#) and [b](#); data available in [Table 1](#)). The thermal conductivities of the sandstone and limestone were reduced from  $\sim 3.9$  to  $\sim 3.5 \text{ W}\cdot\text{m}^{-1}\cdot\text{K}^{-1}$  and from  $\sim 1.9$  to  $\sim 1.2 \text{ W}\cdot\text{m}^{-1}\cdot\text{K}^{-1}$ , respectively, as temperature was increased ([Fig. 3a](#) and [b](#)). The measured decrease in thermal conductivity measured in Fontainebleau sandstone and Indiana limestone is similar to previously published data for sandstones and limestones ([Clauser and Huenges, 1995](#); [Vosteen and Schellschmidt, 2003](#); [Abdulagatova et al., 2009](#); [Merriman et al., 2018](#); [Norden et al., 2020](#); [Chen et al., 2021](#); [Emirov et al., 2021](#)) and is a consequence of the large decrease in the thermal conductivity of quartz ([Clauser and Huenges, 1995](#)) and calcite ([Merriman et al., 2018](#)) as a function of temperature, due to a decrease in lattice thermal conductivity. At temperatures up to 120 °C, we only expect very few, if any, thermal microcracks to form in sandstone ([Sirdesai et al., 2019](#)) and limestone ([Jodry et al., 2023](#)), which would serve to reduce the thermal conductivity of rock ([Kant et al., 2017](#); [Zhao et al., 2018](#)). We also note that 120 °C is below the temperature required for the thermal decomposition of calcite, which occurs at temperatures  $> 650$  °C ([Heap et al., 2013](#)).

## 3. Results

The thermal conductivity of our andesite samples is plotted as a function of connected porosity and temperature in [Fig. 4a](#) and [b](#), respectively (data available in [Table 2](#)). The data are colour-coded in [Fig. 4a](#) and [b](#) to show, respectively, the temperature (with blue and red indicating low and high temperature, respectively) and the porosity (with black and white indicating low and high porosity, respectively). [Fig. 5](#) replots the data in [Fig. 4b](#) so that the evolution of thermal conductivity as a function of temperature can be observed more clearly. We first note that, at room temperature, the thermal conductivity decreases from  $\sim 1.6$  to  $\sim 0.4 \text{ W}\cdot\text{m}^{-1}\cdot\text{K}^{-1}$  as porosity is increased from  $\sim 0.05$  to

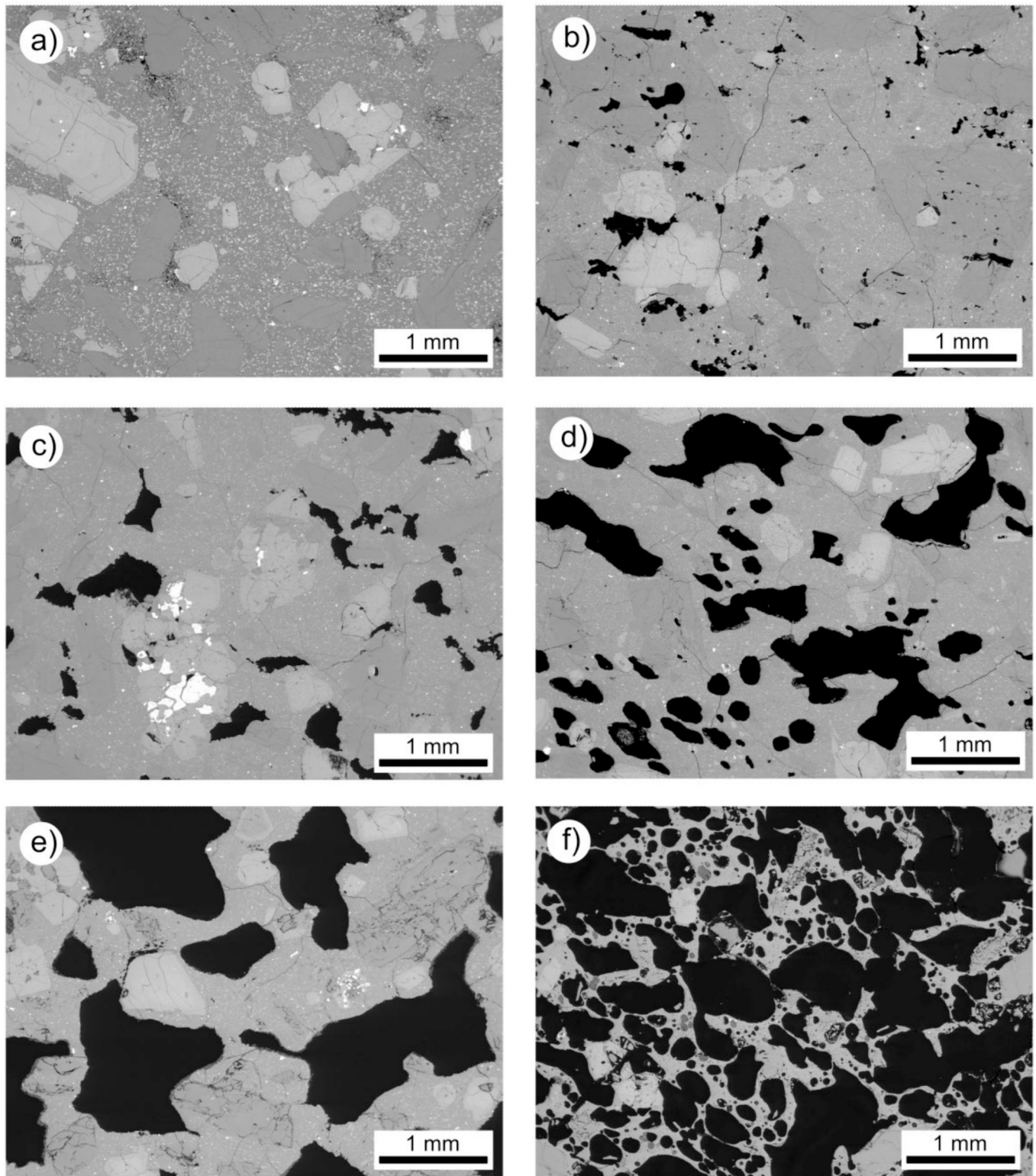


**Fig. 1.** Scanning electron microscope images, in backscatter mode, of six of the andesites from Mt. Ruapehu used for this study. (a) Sample R3, with an average connected porosity of 0.04 with abundant microlites. (b) Sample R6, with an average connected porosity of 0.05 and microlite-rich groundmass. (c) Sample R8, with an average connected porosity of 0.11 and microlite-rich groundmass. (d) Sample R10, with an average connected porosity of 0.16 and microlite-rich groundmass. (e) Sample R14, with an average connected porosity of 0.33 and microlite-rich groundmass. (f) Sample R17, with an average connected porosity of 0.62 and microlite-poor groundmass.

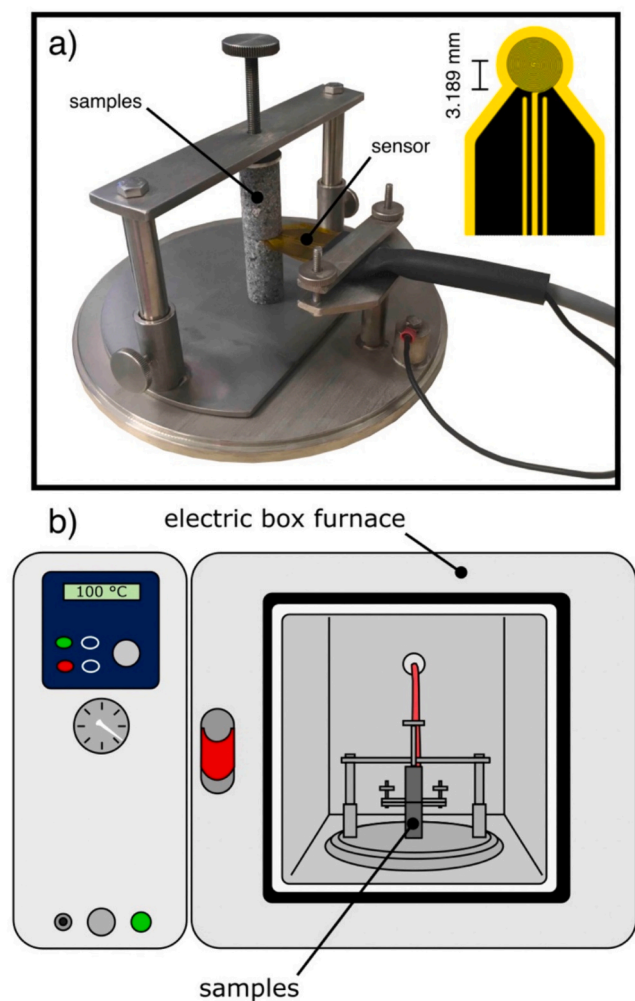


**Fig. 2.** (a) Photograph of the experimental setup for the measurements. Inset shows the sensor used, consisting of two 10  $\mu\text{m}$ -thick nickel foil spirals (radius of 3.189 mm) that are encased and insulated by 30  $\mu\text{m}$ -thick kapton. The screw on the top of the setup ensures a good contact between the sensor and the samples. (b) Schematic diagram showing the measurement setup for this study. The entire experimental setup shown in panel (a) was placed inside an electric box furnace for the measurements performed for this study.

$\sim 0.6$  (Fig. 4a; Table 2). Figs. 4 and 5 also show that (1) the thermal conductivity of the andesites does not change appreciably within the range of temperatures tested and (2) porosity (in the range  $\sim 0.05$ – $0.6$ ) does not influence the temperature dependence of thermal conductivity. In detail, Fig. 5 shows that the thermal conductivity either remains more-or-less constant as a function of temperature, or decreases very slightly, and that, in general, the samples for which thermal conductivity decreases slightly are those with lower porosities. However, we note that the magnitude of any reductions in thermal conductivity as temperature is increased is very close to the standard deviations of the measurements (Fig. 5).

#### 4. Discussion

Our data show that the thermal conductivity of our andesite samples decreases from  $\sim 1.6$  to  $\sim 0.4 \text{ W}\cdot\text{m}^{-1}\cdot\text{K}^{-1}$  as porosity is increased from  $\sim 0.05$  to  $\sim 0.6$  (Fig. 4a), in agreement with previously published data (Robertson and Peck, 1974; Heap et al., 2020, 2022) and modelling (Keszthelyi, 1994) for volcanic rocks, and can be explained by the significantly lower thermal conductivity of the air that fills the void space compared to the minerals that form these rocks.

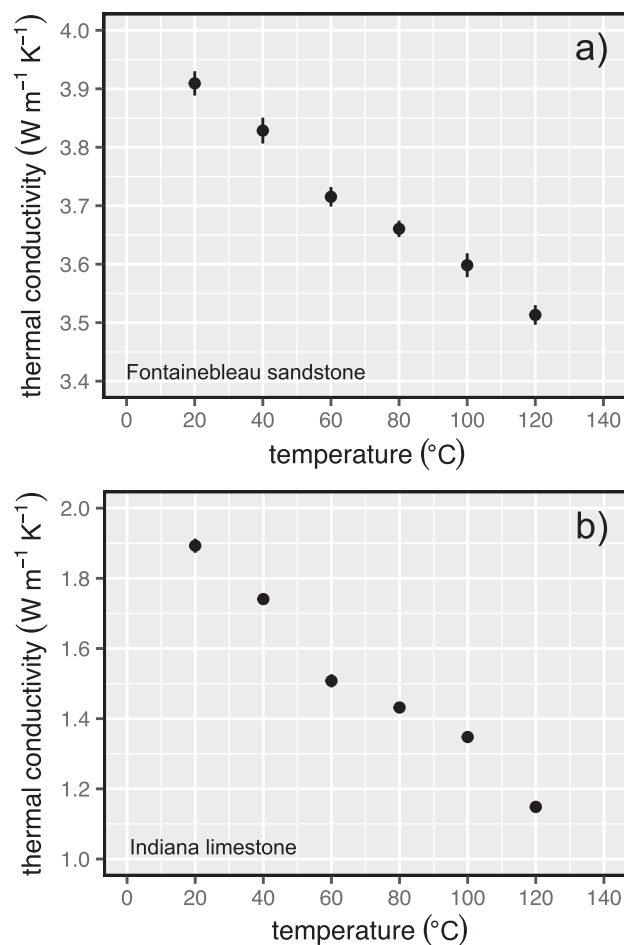


**Fig. 3.** Thermal conductivity as a function of temperature for (a) Fontainebleau sandstone and (b) Indiana limestone. Data available in Table 1.

**Table 1**  
Thermal conductivity of Fontainebleau sandstone (FTB) and Indiana limestone (IL) as a function of temperature.

Sample number	Connected porosity	Temperature (°C)	Thermal conductivity ( $\text{W}\cdot\text{m}^{-1}\cdot\text{K}^{-1}$ )
FTB	0.05	20	$3.91 \pm 0.021$
FTB	0.05	40	$3.83 \pm 0.022$
FTB	0.05	60	$3.72 \pm 0.017$
FTB	0.05	80	$3.66 \pm 0.014$
FTB	0.05	100	$3.60 \pm 0.021$
FTB	0.05	120	$3.51 \pm 0.017$
IL	0.16	20	$1.89 \pm 0.020$
IL	0.16	40	$1.74 \pm 0.015$
IL	0.16	60	$1.51 \pm 0.019$
IL	0.16	80	$1.43 \pm 0.011$
IL	0.16	100	$1.35 \pm 0.009$
IL	0.16	120	$1.15 \pm 0.013$

We also provide the connected porosity of each sample pair. The thermal conductivity of each sample pair was measured four times and we report the mean and standard deviation of the mean of these four measurements.

However, in contrast to the data for the sedimentary rocks (Fig. 3), the thermal conductivity of our andesite samples either did not change appreciably or decreased very slightly as a function of temperature (Figs. 4 and 5). Although the thermal conductivity data presented here using the TPS method may not be as accurate as, for example, measurements provided using the LFA method, adding some uncertainty to our data, we highlight that our device is capable of measuring the expected decrease in thermal conductivity in sandstone and limestone as a

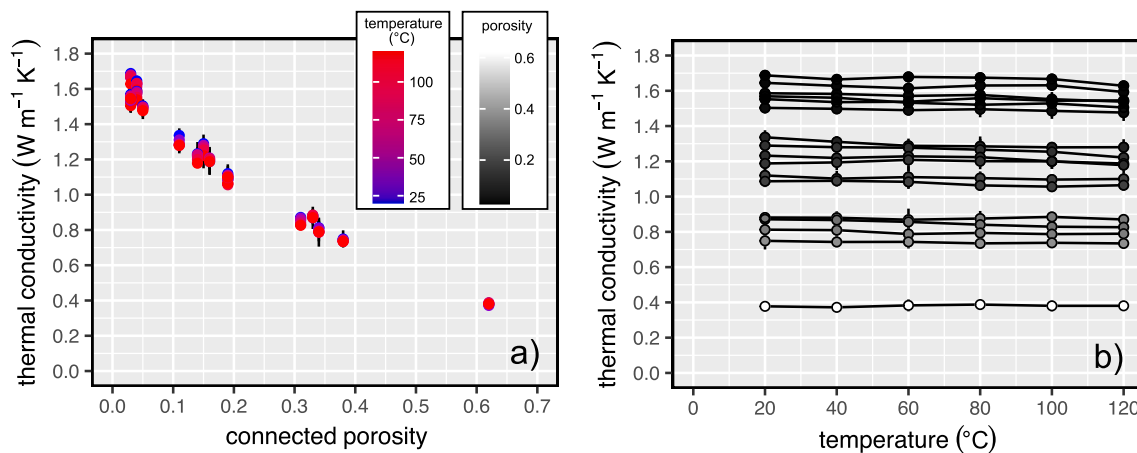


**Fig. 4.** (a) Thermal conductivity as a function of connected porosity for a suite of andesites from Mt. Ruapehu. Symbols are coloured so that measurements made at high and low temperature are shown in red and blue, respectively. (b) Thermal conductivity as a function of temperature for the same suite of andesites shown in panel (a). Symbols are coloured so that high- and low-porosity (connected porosity) samples are shown in black and white, respectively (colour scale bar shown on panel (a)). Data available in Table 2. (For interpretation of the references to colour in this figure legend, the reader is referred to the web version of this article.)

function of temperature (Fig. 3). Therefore, although we cannot be absolutely certain as to whether there is a very slight increase or decrease in the thermal conductivity of our andesite samples as a function of temperature, we can conclude with some certainty that their thermal conductivity does not change appreciably up to 120 °C, as also observed for andesite from Mt. Shasta up to a temperature of almost 900 °C using the LFA method (Hofmeister, 2020; Fig. 6).

Here, we compile published data for the thermal conductivity of volcanic rocks as a function of temperature, which show that (1) the thermal conductivity of tuff and some basalts decreases as a function of temperature, (2) the thermal conductivity of some basalts, some diabases, and an andesite does not appreciably or systematically change as a function of temperature, and (3) that the thermal conductivity of obsidian and a range of glasses of different compositions increases as a function of temperature (see the data compilations presented in Desai et al., 1974; Čermák and Rybach, 1982; Clauser and Huenges, 1995; Hofmeister et al., 2016). We show these compiled data, and more recent data, in Fig. 7. We have split the published data into three groups (1) rocks for which thermal conductivity decreases as temperature is increased (Fig. 7a), (2) rocks for which thermal conductivity does not appreciably change or increases and then decreases (Fig. 7b), and (3) rocks for which thermal conductivity increases (Fig. 7c). Therefore, our data for our andesite samples (Figs. 4 and 5) are in agreement with those data in Fig. 7b, including the data for andesite from Mt. Shasta from Hofmeister (2020). The decreases in thermal conductivity as a function of temperature for the rocks in Fig. 7a are much more significant than observed in our data (Figs. 4 and 5).

Key to understanding the different temperature dependency of thermal conductivity of different volcanic rocks (Fig. 7) is the difference between the evolution of thermal conductivity in crystalline and amorphous materials as a function of temperature (e.g., Zhou et al., 2020). The thermal conductivity of amorphous materials, such as amorphous glass, increases as a function of temperature, whereas the thermal conductivity of crystalline materials decreases. For example, the thermal conductivity of amorphous silica glass increases systematically as a function of temperature, from  $\sim 1.36 \text{ W}\cdot\text{m}^{-1}\cdot\text{K}^{-1}$  at 0 °C to  $\sim 2.07 \text{ W}\cdot\text{m}^{-1}\cdot\text{K}^{-1}$  at a temperature of 500 °C (Clauser and Huenges, 1995). Hofmeister et al. (2016) also show that the thermal conductivity of a wide range of glasses with different compositions increase as a function of increasing temperature (Fig. 7c). It is for this reason why the rocks for which thermal conductivity increases with increasing temperature (Fig. 7c) are all glassy or glass. To complement these data, and to help further validate our setup and method, we measured the thermal conductivity of microlite-free obsidian from Hrafninnuhryggur (Krafla

volcano, Iceland; Tuffen and Castro, 2009) using the same approach and conditions described in our methods section. For these measurements, the output power and test duration used were 180 mW and 10 s, respectively. Our data show that the thermal conductivity of the obsidian increases as a function of temperature, from  $\sim 1.34$  to  $\sim 1.44 \text{ W}\cdot\text{m}^{-1}\cdot\text{K}^{-1}$  (Fig. 8; data available in Table 3), in accordance with other data for obsidian and other glasses (Fig. 7c). The increase in thermal conductivity as a function of temperature for the obsidian from Hrafninnuhryggur (Fig. 8) is higher than that measured for obsidian from Mono Craters (California, USA) by Romine et al. (2012). Using the LFA method, Romine et al. (2012) showed that the thermal conductivity of obsidian from Mono Craters increased from  $\sim 1.15 \text{ W}\cdot\text{m}^{-1}\cdot\text{K}^{-1}$  at room temperature to  $\sim 1.22 \text{ W}\cdot\text{m}^{-1}\cdot\text{K}^{-1}$  at a temperature of 120 °C. The difference between the two datasets could be the result of the presence of microlites in the samples from Mono Craters (Romine et al., 2012).

Therefore, the variable temperature dependencies of thermal conductivity of different volcanic rocks (Fig. 7) can be explained by variable quantities of amorphous and crystalline material. Volcanic rocks for which thermal conductivity decreases (Fig. 7a) are those devoid of amorphous glass, and those for which thermal conductivity does not appreciably change, or change systematically (Fig. 7b), are those that contain a mixture of amorphous glass and crystalline materials. These assertions are in line with the typical glass contents of the various rock types for which data exist (Fig. 7) and, where available, the descriptions of the rocks in the published literature. For example, although fresh rhyolites are often glassy, the data shown in Fig. 7a are for rhyolites that are more than two billion years old and are, therefore, extremely unlikely to contain any glass (Ray et al., 2023).

We test for the effects hypothesised here by considering the relative phase proportions of amorphous and crystalline material in a given sample and attributing a weighted contribution of each material to the bulk thermal conductivity. We do this by assigning a temperature dependence of thermal conductivity to the amorphous (glass) phase,  $\lambda_g(T)$ , and to the crystalline phase,  $\lambda_c(T)$ , and then simply applying a weighted combination to give the total conductivity as  $\lambda = \lambda_g(1 - \phi_c) + \lambda_c\phi_c$ , where  $\phi_c$  is the volume fraction of the solid that is crystalline. Additionally, this mixture model can then be taken to be porosity dependent through the choice of model for  $\lambda_g$  and  $\lambda_c$ . Inspection of Fig. 7 shows that these contributions should be approximately linear over the temperature interval used here, such that  $\lambda_g(T) = aT + \lambda'_g$  and  $\lambda_c(T) = bT + \lambda'_c$ , and where  $a$  and  $b$  are best-fit coefficients for the temperature dependence of the thermal conductivity, and  $\lambda'_g$  and  $\lambda'_c$  are the conductivities at a given reference temperature (taken here to be 0 °C). By

**Table 2**

Thermal conductivity of the 17 andesites collected at Mt. Ruapehu as a function of temperature.

Sample number	Connected porosity	Temperature (°C)	Thermal conductivity (W·m <sup>-1</sup> ·K <sup>-1</sup> )
R1	0.03	20	1.69 ± 0.022
R1	0.03	40	1.66 ± 0.027
R1	0.03	60	1.68 ± 0.019
R1	0.03	80	1.67 ± 0.027
R1	0.03	100	1.67 ± 0.017
R1	0.03	120	1.63 ± 0.015
R2	0.03	20	1.57 ± 0.052
R2	0.03	40	1.56 ± 0.072
R2	0.03	60	1.53 ± 0.031
R2	0.03	80	1.52 ± 0.052
R2	0.03	100	1.53 ± 0.064
R2	0.03	120	1.51 ± 0.032
R3	0.04	20	1.65 ± 0.030
R3	0.04	40	1.63 ± 0.010
R3	0.04	60	1.61 ± 0.029
R3	0.04	80	1.63 ± 0.025
R3	0.04	100	1.63 ± 0.023
R3	0.04	120	1.59 ± 0.037
R4	0.04	20	1.59 ± 0.021
R4	0.04	40	1.58 ± 0.010
R4	0.04	60	1.57 ± 0.011
R4	0.04	80	1.58 ± 0.019
R4	0.04	100	1.55 ± 0.011
R4	0.04	120	1.54 ± 0.030
R5	0.03	20	1.55 ± 0.021
R5	0.03	40	1.54 ± 0.024
R5	0.03	60	1.54 ± 0.008
R5	0.03	80	1.56 ± 0.015
R5	0.03	100	1.54 ± 0.013
R5	0.03	120	1.55 ± 0.041
R6	0.05	20	1.50 ± 0.031
R6	0.05	40	1.50 ± 0.022
R6	0.05	60	1.49 ± 0.025
R6	0.05	80	1.50 ± 0.046
R6	0.05	100	1.49 ± 0.045
R6	0.05	120	1.48 ± 0.048
R7	0.19	20	1.09 ± 0.033
R7	0.19	40	1.09 ± 0.022
R7	0.19	60	1.08 ± 0.040
R7	0.19	80	1.06 ± 0.024
R7	0.19	100	1.06 ± 0.029
R7	0.19	120	1.06 ± 0.030
R8	0.11	20	1.34 ± 0.040
R8	0.11	40	1.31 ± 0.032
R8	0.11	60	1.29 ± 0.041
R8	0.11	80	1.29 ± 0.042
R8	0.11	100	1.28 ± 0.023
R8	0.11	120	1.28 ± 0.045
R9	0.15	20	1.29 ± 0.030
R9	0.15	40	1.28 ± 0.032
R9	0.15	60	1.28 ± 0.019
R9	0.15	80	1.27 ± 0.075
R9	0.15	100	1.25 ± 0.039
R9	0.15	120	1.22 ± 0.072
R10	0.16	20	1.19 ± 0.071
R10	0.16	40	1.19 ± 0.044
R10	0.16	60	1.21 ± 0.063
R10	0.16	80	1.20 ± 0.046
R10	0.16	100	1.20 ± 0.042
R10	0.16	120	1.19 ± 0.075
R11	0.14	20	1.23 ± 0.067
R11	0.14	40	1.22 ± 0.024
R11	0.14	60	1.23 ± 0.041
R11	0.14	80	1.22 ± 0.036
R11	0.14	100	1.20 ± 0.043
R11	0.14	120	1.18 ± 0.018
R12	0.19	20	1.12 ± 0.042
R12	0.19	40	1.10 ± 0.044
R12	0.19	60	1.11 ± 0.062
R12	0.19	80	1.10 ± 0.038
R12	0.19	100	1.10 ± 0.031
R12	0.19	120	1.10 ± 0.019

**Table 2 (continued)**

Sample number	Connected porosity	Temperature (°C)	Thermal conductivity (W·m <sup>-1</sup> ·K <sup>-1</sup> )
R13	0.31	20	0.87 ± 0.018
R13	0.31	40	0.87 ± 0.019
R13	0.31	60	0.86 ± 0.010
R13	0.31	80	0.84 ± 0.004
R13	0.31	100	0.83 ± 0.014
R13	0.31	120	0.83 ± 0.007
R14	0.33	20	0.88 ± 0.028
R14	0.33	40	0.88 ± 0.036
R14	0.33	60	0.87 ± 0.063
R14	0.33	80	0.88 ± 0.043
R14	0.33	100	0.88 ± 0.027
R14	0.33	120	0.87 ± 0.021
R15	0.34	20	0.81 ± 0.040
R15	0.34	40	0.81 ± 0.055
R15	0.34	60	0.79 ± 0.082
R15	0.34	80	0.79 ± 0.058
R15	0.34	100	0.79 ± 0.003
R15	0.34	120	0.79 ± 0.031
R16	0.38	20	0.75 ± 0.049
R16	0.38	40	0.74 ± 0.015
R16	0.38	60	0.74 ± 0.028
R16	0.38	80	0.73 ± 0.021
R16	0.38	100	0.74 ± 0.006
R16	0.38	120	0.73 ± 0.013
R17	0.62	20	0.38 ± 0.017
R17	0.62	40	0.37 ± 0.018
R17	0.62	60	0.38 ± 0.034
R17	0.62	80	0.39 ± 0.022
R17	0.62	100	0.38 ± 0.032
R17	0.62	120	0.38 ± 0.023

We also provide the average connected porosity of each sample pair. The thermal conductivity of each sample pair was measured four times and we report the mean and standard deviation of the mean of these four measurements.

injecting these two linear temperature-dependent laws into the model for  $\lambda$ , we can thus test the hypothesis that some intermediate crystallinity  $\phi_c^*$  can explain the apparent lack of temperature dependence for the andesites measured herein (Fig. 4b), and also for the rocks shown in Fig. 7b. Thus the model is given by:

$$\lambda = (aT + \lambda'_g) (1 - \phi_c) + (bT + \lambda'_c) \phi_c \quad (1)$$

In line with our microstructural observations (Fig. 1), Eq. (1) assumes an isotropic medium, a mixture comprising isotropic inclusions of one phase embedded within a second phase. We note that solutions for anisotropic media, and solutions for isotropic media that consider the mean of two end-member anisotropic solutions to thermal properties, are available in Merriman et al. (2023).

We can estimate the critical crystalline content, i.e.  $\phi_c^*$ , required for a temperature-independent model by setting  $\partial\lambda/\partial T = b\phi_c + a(1 - \phi_c)$  to zero and solving to find  $\phi_c^* = a/(a - b)$ . To find  $a$  and  $b$ , we use the average temperature dependence of the thermal conductivity for the completely glassy materials and the fully crystalline materials shown in Fig. 7c and a, respectively. To find the coefficients, we use a least squares minimisation following Kemmer and Keller (2010). We find that  $a = 0.0006 \text{ W}\cdot\text{m}^{-1}\cdot\text{°C}^{-2}$  and  $b = -0.00172 \text{ W}\cdot\text{m}^{-1}\cdot\text{°C}^{-2}$ . In doing so, we find  $\phi_c^* \approx 0.26$ , as shown in Fig. 9. To capture the variability in the collated data (Fig. 7a and c), and therefore our crystallinity predictions, we also provide estimations for the minimum and maximum values for  $\phi_c^*$ , using the minimum ( $a = 0.0002 \text{ W}\cdot\text{m}^{-1}\cdot\text{°C}^{-2}$  and  $b = -0.0036 \text{ W}\cdot\text{m}^{-1}\cdot\text{°C}^{-2}$ ) and maximum ( $a = 0.0014 \text{ W}\cdot\text{m}^{-1}\cdot\text{°C}^{-2}$  and  $b = -0.0005 \text{ W}\cdot\text{m}^{-1}\cdot\text{°C}^{-2}$ ) values for  $a$  and  $b$  from the collated dataset. Using these values, we find a minimum and maximum value for  $\phi_c^*$  of 0.05 and 0.74, respectively (Fig. 9). We note that the range of predicted crystallinities for a temperature-independent thermal conductivity is not dissimilar to estimates of the crystallinity of dome lava andesites. For example, the crystallinities of andesites from Volcán de Colima (Mexico), Anak

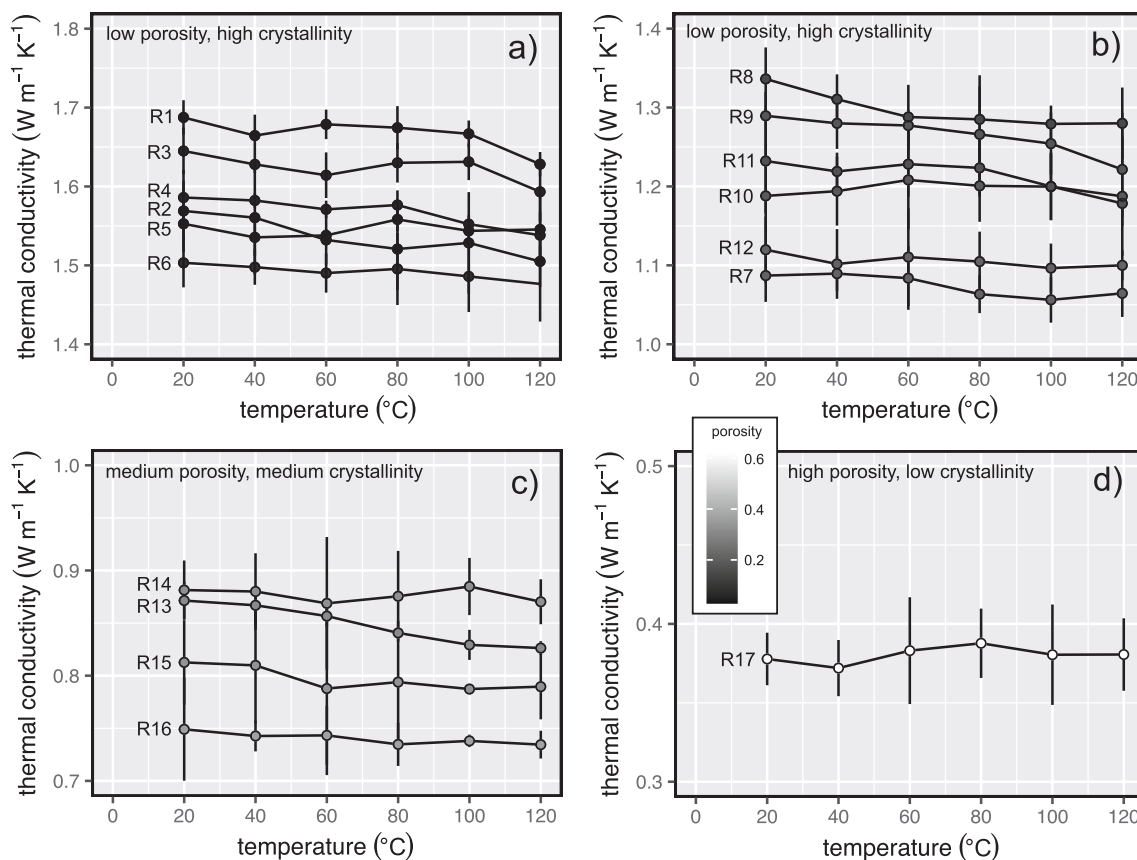


**Fig. 5.** (a) Thermal conductivity as a function of temperature for a suite of andesites from Mt. Ruapehu (the same data shown in Fig. 4). (a) Data for R1 – R6. (b) Data for R7 – R12. (c) Data for R13 – R16. (d) Data for R17. Symbols are coloured so that high- and low-porosity samples are shown in black and white, respectively (colour scale bar shown on panel (d)). Data available in Table 2.

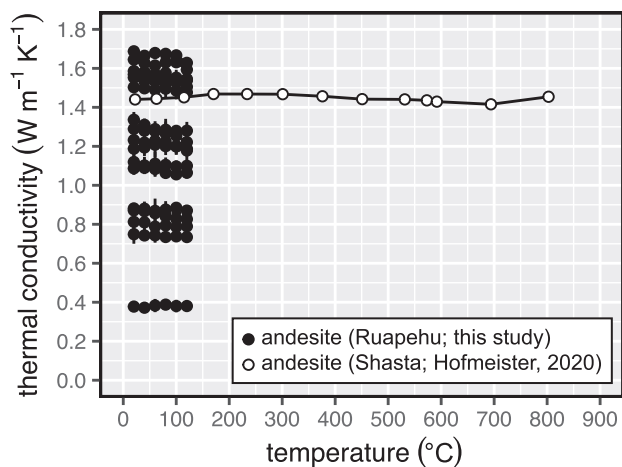


**Fig. 6.** Thermal conductivity as a function of temperature for the andesites measured for this study (from Mt. Ruapehu, New Zealand) and an andesite sample from Mt. Shasta (USA; data from Hofmeister, 2020).

Krakatau (Indonesia), and Bezymianny (Russia) were estimated to be 40, 50, and 70%, respectively (Lavallée et al., 2007).

Values of thermal conductivity for rocks at the predicted  $\phi_c^*$  could be provided using Eq. (1) as long as  $\lambda_g^*$  and  $\lambda_c^*$  are known and, because the current model does not account for porosity, the rock has a porosity of zero. The effect of porosity would be to lower the predicted thermal conductivity, as highlighted in Fig. 4. Additionally, the reference conductivity  $\lambda_c^*$  plays a role and could be different for the dense rock

equivalent andesite groundmass and phenocrysts.

Based on the above reasoning, in order to explain the more-or-less temperature-independent thermal conductivity (Figs. 4 and 5), our andesites should contain a mixture of amorphous glass and crystalline materials. Indeed, our microstructural observations show that our andesites are characterised by phenocrysts hosted within a variably glassy groundmass (Fig. 1). We therefore suggest that the thermal conductivity of these andesites did not appreciably change up to a temperature of 120 °C because the decrease in the thermal conductivity of the crystalline materials, due to decreases in lattice thermal conductivity, was offset by the increase in thermal conductivity of the amorphous glass. The fact that we observe slight decreases in thermal conductivity as a function of temperature for some of the low-porosity samples, the samples that have more abundant microlites, also supports this hypothesis, although we again note that the magnitude of these decreases is close to the standard deviations of these measurements (Fig. 5). Finally, we highlight that we only expect very few, if any, thermal microcracks to form in our andesites at temperatures up to 120 °C. For example, Heap et al. (2018) found that the physical properties of similar andesite, from Volcán de Colima (Mexico), did not change following exposure to 900 °C.

We highlight that our laboratory measurements were performed on oven-dry samples at ambient pressure. Higher pressures and saturation with water, corresponding to common conditions in volcanic hydrothermal and geothermal systems, would serve to increase the thermal conductivity values provided herein (Walsh and Decker, 1966). Although not possible in our current experimental setup, we note that small increases in the thermal conductivity of our andesites as a function of temperature may have been observed below the boiling point of water if the samples had been water-saturated. This is because the thermal

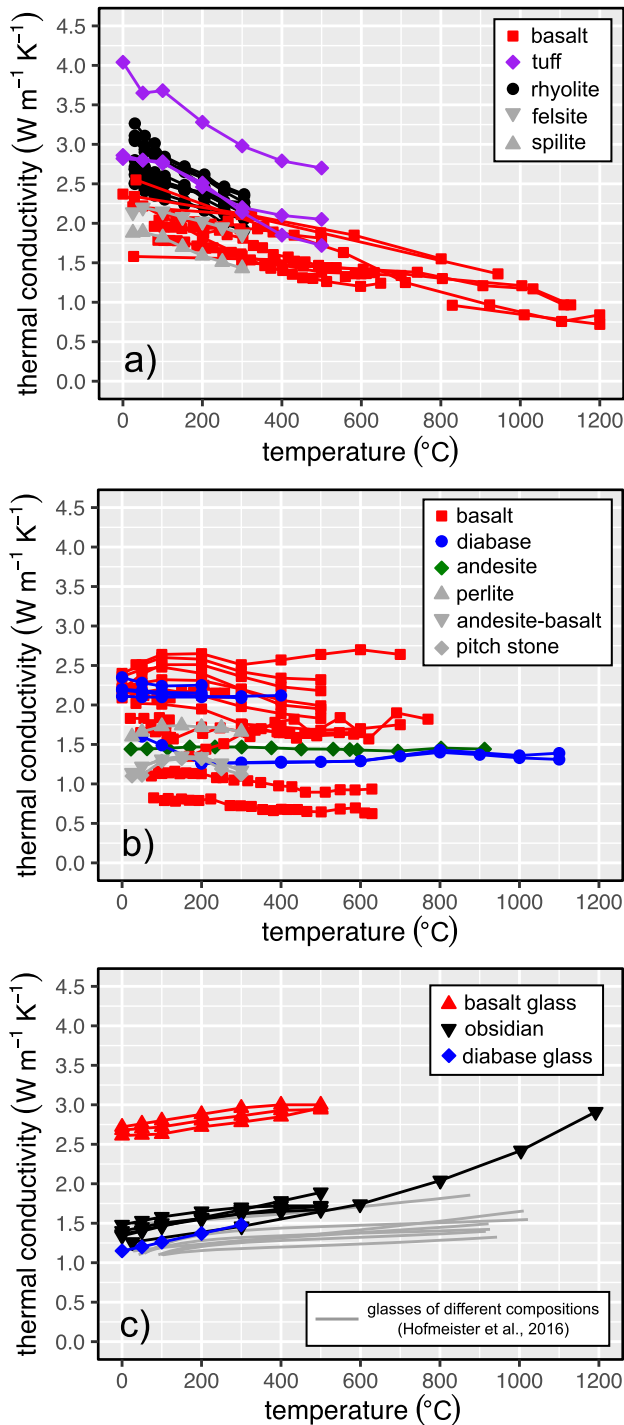


**Fig. 7.** (a) Thermal conductivity as a function of temperature for volcanic rocks. (a) Rocks for which thermal conductivity decreases as temperature increases. (b) Rocks for which thermal conductivity does not appreciably change or increases and then decreases as temperature increases. (c) Rocks for which thermal conductivity increases as temperature increases. Data from Desai et al. (1974), Čermák and Rybach (1982), Mostafa et al. (2004), Hofmeister et al. (2016), Nahhas et al. (2019), Hofmeister (2020), Chen et al. (2021), and Ray et al. (2023).

conductivity of water increases slightly as a function of temperature, from  $\sim 0.6 \text{ W}\cdot\text{m}^{-1}\cdot\text{K}^{-1}$  at room temperature to  $\sim 0.68 \text{ W}\cdot\text{m}^{-1}\cdot\text{K}^{-1}$  at a temperature of  $100 \text{ }^\circ\text{C}$  (Sharqawy, 2013). We also highlight that, although our data show that the thermal conductivity of a suite of andesites is unchanged at temperatures up to  $120 \text{ }^\circ\text{C}$ , we urge caution. The

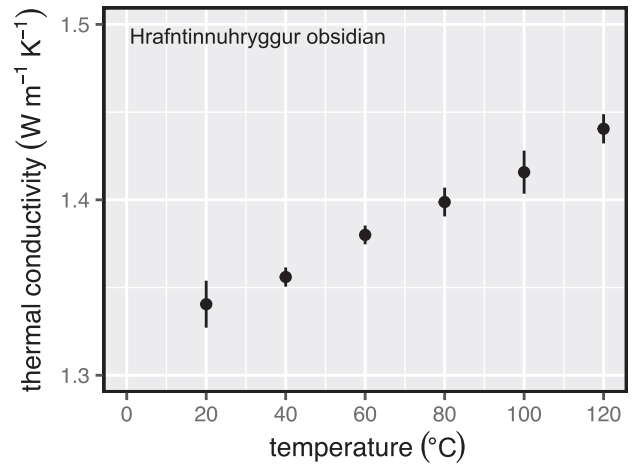


**Fig. 8.** Thermal conductivity as a function of temperature for obsidian from Hrafninnuhryggur (Krafla, Iceland). Data available in Table 3.

**Table 3**

Thermal conductivity of Hrafninnuhryggur obsidian (HO) as a function of temperature.

Sample number	Connected porosity	Temperature ( $^\circ\text{C}$ )	Thermal conductivity ( $\text{W}\cdot\text{m}^{-1}\cdot\text{K}^{-1}$ )
HO	0.00	20	$1.34 \pm 0.013$
HO	0.00	40	$1.36 \pm 0.005$
HO	0.00	60	$1.38 \pm 0.005$
HO	0.00	80	$1.40 \pm 0.005$
HO	0.00	100	$1.42 \pm 0.012$
HO	0.00	120	$1.44 \pm 0.008$

We also provide the average connected porosity of the two HO samples. The thermal conductivity of each sample pair was measured four times and we report the mean and standard deviation of the mean of these four measurements.

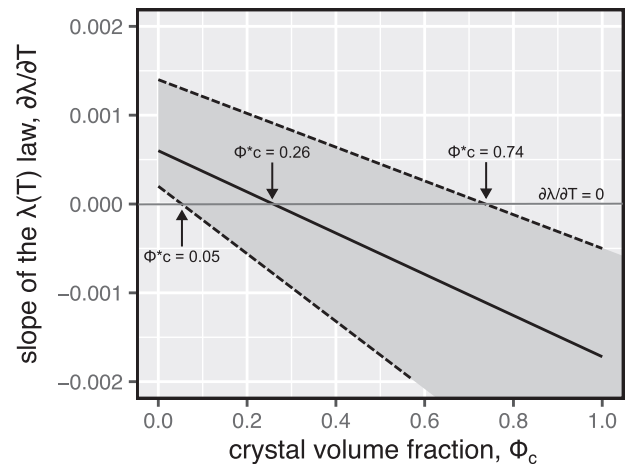


**Fig. 9.**  $\partial\lambda/\partial T$  (the derivative of  $\lambda$  in Eq. (1) with respect to temperature) as a function of crystal volume fraction,  $\phi_c$ . The solid line uses the average values for  $a$  and  $b$  from the collated dataset (i.e., Fig. 7c and a), and the dashed lines use the minimum and maximum values for  $a$  and  $b$  from the collated dataset. Where these lines cross the  $\partial\lambda/\partial T = 0$  line provides the estimate for  $\phi_c^*$ . See text for details.

thermal conductivity other andesites that contain less or more glass may decrease or increase, respectively, as a function of temperature. We suggest that more experimental studies are now required to assess the evolution of thermal conductivity as a function of temperature in a wide range of volcanic rocks with different crystallinities. Finally, based on

the compiled data for volcanic rocks (Fig. 7), and our new data (Figs. 4 and 5), we highlight that the empirical temperature correction functions, typically employed for granitic and sedimentary rocks (Norden et al., 2020), are likely unsuitable for volcanic rocks. However, our study provides the first steps towards a robust empirical relationship for volcanic rocks.

## 5. Conclusions

The thermal conductivity of granitic and sedimentary rocks decreases systematically as a function of increasing temperature (Desai et al., 1974; Čermák and Rybach, 1982; Clauser and Huenges, 1995; Vosteen and Schellschmidt, 2003; Norden et al., 2020; Clauser, 2021). This is because these rocks typically contain minerals, such as quartz, calcite, and dolomite, for which thermal conductivity decreases significantly as temperature is increased (Clauser and Huenges, 1995; Meriman et al., 2018). Volcanic rocks, however, do not typically contain these minerals, although some rhyolites can contain abundant quartz (e. g., Toyoda et al., 1995; Shane et al., 2008; Graeter et al., 2015). Volcanic rocks exist on a spectrum between completely glassy and completely crystallised or devitrified and, because the thermal conductivity of amorphous glass and crystalline materials increase and decrease, respectively, as a function of temperature, the temperature dependence of their thermal conductivity depends on where they lie on this spectrum. Therefore, (1) the thermal conductivity of volcanic rocks devoid of glass (i.e. those completely crystallised or devitrified) decreases with increasing temperature (Fig. 7a), (2) the thermal conductivity of completely glassy volcanic rocks increases with increasing temperature (Fig. 7c), and (3) the thermal conductivity of volcanic rocks containing mixtures of amorphous glass and crystalline materials remains more-or-less constant with increasing temperature (Fig. 7b). The thermal conductivity of the andesites measured herein, which contain phenocrysts hosted within a variably glassy groundmass (Fig. 1), did not appreciably change as a function of temperature (Figs. 4 and 5). This is because decreases in thermal conductivity due to the presence of crystalline materials was offset by increases due to the presence of amorphous glass. A simple model, using the average temperature dependence of the thermal conductivity of the collated data for glass and crystalline material, provides a crystal content of 0.26 for a thermal conductivity independent of temperature, a common value for andesite. Our findings imply that models designed to understand heat transfer in active volcanoes, igneous systems, geothermal reservoirs, and heat storage systems need not consider a temperature-dependent thermal conductivity in partially glassy volcanic rocks, but that decreases and increases in thermal conductivity as a function of temperature should be considered for fully crystallised or devitrified volcanic rocks and completely glassy volcanic rocks, respectively. We conclude that more experimental studies are now required to assess the evolution of thermal conductivity as a function of temperature in a wide range of volcanic rocks with different crystallinities.

## CRedit authorship contribution statement

**Michael J. Heap:** Conceptualization, Formal analysis, Investigation, Resources, Writing – original draft, Visualization, Supervision, Project administration, Funding acquisition. **Gunel Alizada:** Investigation, Writing – review & editing. **David E. Jessop:** Writing – review & editing. **Ben M. Kennedy:** Resources, Writing – review & editing. **Fabian B. Wadsworth:** Formal analysis, Writing – review & editing.

## Declaration of competing interest

The authors declare that there are no conflicts of interest.

## Data availability

All data are provided in the tables presented in the manuscript.

## Acknowledgements

This work of the Interdisciplinary Thematic Institute GeoT, as part of the ITI 2021–2028 program of the University of Strasbourg, CNRS and Inserm, was supported by IdEx Unistra (ANR-10-IDEX-0002), and by SFRI-STRAT'US project (ANR-20-SFRI-0012) under the framework of the French Investments for the Future Program. M. Heap also acknowledges support from the Institut Universitaire de France (IUF). M. Heap was also supported by European Research Council Synergy Grant “ROTTnROCK” (ERC-ROTTnROCK-101118491). A special thanks goes to Harry Keys and Blake McDavitt at the New Zealand Department of Conservation, Ngati Tuwharetoa, Ngati Rangī, and Ruapehu Alpine Lifts for providing access to and permission to sample at Mt. Ruapehu. Kamal Bayramov and Sarvar Mammadov are thanked for their support and assistance. This is Laboratory of Excellence ClerVolc contribution number 613. Ben Kennedy was supported by the NSC Resilience to nature's challenges: “Ahea riri ai ngā maunga puia? When will our volcanoes become angry?” (Ministry of Business, Innovation & Employment). The constructive comments of two reviewers (Sven Fuchs and one anonymous reviewer), and the editor (Shane Cronin), helped improve this manuscript.

## References

- Abdulagatova, Z., Abdulagatov, I.M., Emirov, V.N., 2009. Effect of temperature and pressure on the thermal conductivity of sandstone. *Int. J. Rock Mech. Min. Sci.* 46 (6), 1055–1071.
- Annen, C., 2017. Factors affecting the thickness of thermal aureoles. *Front. Earth Sci.* 5, 82.
- Annen, C., Pichavant, M., Bachmann, O., Burgisser, A., 2008. Conditions for the growth of a long-lived shallow crustal magma chamber below Mount Pelee volcano (Martinique, Lesser Antilles Arc). *J. Geophys. Res. Solid Earth* 113 (B7).
- Arellano, V.M., García, A., Barragán, R.M., Izquierdo, G., Aragón, A., Nieva, D., 2003. An updated conceptual model of the Los Humeros geothermal reservoir (Mexico). *J. Volcanol. Geotherm. Res.* 124 (1–2), 67–88.
- Bagdasarov, N., Dingwell, D., 1994. Thermal properties of vesicular rhyolite. *J. Volcanol. Geotherm. Res.* 60 (2), 179–191.
- Balkan, E., Erkan, K., Şalk, M., 2017. Thermal conductivity of major rock types in western and Central Anatolia regions, Turkey. *J. Geophys. Eng.* 14 (4), 909–919.
- Baud, P., Hall, S., Heap, M.J., Ji, Y., Wong, T.F., 2021. The brittle-ductile transition in porous limestone: failure mode, constitutive modeling of inelastic deformation and strain localization. *J. Geophys. Res. Solid Earth* 126 (5) (e2020JB021602).
- Bourbié, T., Zinszner, B., 1985. Hydraulic and acoustic properties as a function of porosity in Fontainebleau sandstone. *J. Geophys. Res. Solid Earth* 90 (B13), 11524–11532.
- Bruce, P.M., Huppert, H.E., 1989. Thermal control of basaltic fissure eruptions. *Nature* 342 (6250), 665–667.
- Burchardt, S., Bazargan, M., Gestsson, E.B., Hieronymus, C., Ronchin, E., Tuffen, H., Saubin, E., 2022. Geothermal potential of small sub-volcanic intrusions in a typical Icelandic caldera setting. *Volcanica* 5 (2), 477–507.
- Canet, C., Trillaud, F., Prol-Ledesma, R.M., González-Hernández, G., Peláez, B., Hernández-Cruz, B., Sánchez-Córdova, M.M., 2015. Thermal history of the Acoaculco geothermal system, eastern Mexico: insights from numerical modeling and radiocarbon dating. *J. Volcanol. Geotherm. Res.* 305, 56–62.
- Carlino, S., Troiano, A., Di Giuseppe, M.G., Tramelli, A., Troise, C., Somma, R., De Natale, G., 2016. Exploitation of geothermal energy in active volcanic areas: A numerical modelling applied to high temperature Mofete geothermal field, at Campi Flegrei caldera (Southern Italy). *Renew. Energy* 87, 54–66.
- Carrigan, C.R., 1984. Time and temperature dependent convection models of cooling reservoirs: Application to volcanic sills. *Geophys. Res. Lett.* 11 (8), 693–696.
- Carrigan, C.R., Schubert, G., Eichelberger, J.C., 1992. Thermal and dynamical regimes of single- and two-phase magmatic flow in dikes. *J. Geophys. Res. Solid Earth* 97 (B12), 17377–17392.
- Čermák, V., Rybach, L., 1982. Thermal conductivity and specific heat of minerals and rocks. In: Angenheister, G. (Ed.), *Landolt-Börnstein Zahlenwerte und Funktionen aus Naturwissenschaften und Technik, Neue Serie, Physikalische Eigenschaften der Gesteine*, vol. V/1a. Springer Verlag, Berlin, Heidelberg and New York, pp. 305–343.
- Chen, C., Zhu, C., Zhang, B., Tang, B., Li, K., Li, W., Fu, X., 2021. Effect of temperature on the thermal conductivity of rocks and its implication for in situ correction. *Geofluids* 2021, 1–12.
- Chiodini, G., Caliro, S., Avino, R., Bini, G., Giudicepietro, F., De Cesare, W., Tripaldi, S., 2021. Hydrothermal pressure-temperature control on CO<sub>2</sub> emissions and seismicity at Campi Flegrei (Italy). *J. Volcanol. Geotherm. Res.* 414, 107245.

- Clauser, C., 2021. Thermal storage and transport properties of rocks, II: Thermal conductivity and diffusivity. In: *Encyclopedia of Solid Earth Geophysics*. Springer International Publishing, Cham, pp. 1769–1787.
- Clauser, C., Huenges, E., 1995. Thermal conductivity of rocks and minerals. In: *Rock Physics and Phase Relations: A Handbook of Physical Constants*, 3, pp. 105–126.
- Desai, P.D., Navarro, R.A., Hasan, S.E., Ho, C.Y., DeWitt, D.P., West, T.R., 1974. *Thermophysical Properties of Selected Rocks*. Center for Information and Numerical Data Analysis and Synthesis, TPRC Report, p. 23.
- Emirov, S.N., Aliverdiev, A.A., Zarichnyak, Y.P., Emirov, R.M., 2021. Studies of the effective thermal conductivity of sandstone under high pressure and temperature. *Rock Mech. Rock. Eng.* 54, 3165–3174.
- Fialko, Y.A., Rubin, A.M., 1999. Thermal and mechanical aspects of magma emplacement in giant dike swarms. *J. Geophys. Res. Solid Earth* 104 (B10), 23033–23049.
- Fujii, N., Osako, M., 1973. Thermal diffusivity of lunar rocks under atmospheric and vacuum conditions. *Earth Planet. Sci. Lett.* 18 (1), 65–71.
- Girona, T., Realmuto, V., Lundgren, P., 2021. Large-scale thermal unrest of volcanoes for years prior to eruption. *Nat. Geosci.* 14 (4), 238–241.
- González, J., Zambra, C.E., González, L., Clausen, B., Vasco, D.A., 2022. Simulation of cooling in a magma chamber: Implications for geothermal fields of southern Peru. *Geothermics* 105, 102515.
- Graeter, K.A., Beane, R.J., Deering, C.D., Gravley, D., Bachmann, O., 2015. Formation of rhyolite at the Okataina Volcanic complex, New Zealand: New insights from analysis of quartz clusters in plutonic lithics. *Am. Mineral.* 100 (8–9), 1778–1789.
- Gunnarsson, G., Aradóttir, E.S., 2015. The deep roots of geothermal systems in volcanic areas: boundary conditions and heat sources in reservoir modeling. *Transp. Porous Media* 108, 43–59.
- Gustafsson, S.E., 1991. Transient plane source techniques for thermal conductivity and thermal diffusivity measurements of solid materials. *Rev. Sci. Instrum.* 62 (3), 797–804.
- Hammerschmidt, U., Sabuga, W., 2000. Transient hot strip (THS) method: uncertainty assessment. *Int. J. Thermophys.* 21, 217–248.
- Harl, P., Kushnir, A.R., Aichholzer, C., Heap, M.J., Hehn, R., Maurer, V., Düringer, P., 2019. Heat flow density estimates in the Upper Rhine Graben using laboratory measurements of thermal conductivity on sedimentary rocks. *Geotherm. Energy* 7 (1), 1–36.
- Heap, M.J., Kennedy, B.M., 2016. Exploring the scale-dependent permeability of fractured andesite. *Earth Planet. Sci. Lett.* 447, 139–150.
- Heap, M.J., Mollo, S., Vinciguerra, S., Lavallée, Y., Hess, K.U., Dingwell, D.B., Iezzi, G., 2013. Thermal weakening of the carbonate basement under Mt. Etna volcano (Italy): Implications for volcano instability. *J. Volcanol. Geotherm. Res.* 250, 42–60.
- Heap, M.J., Coats, R., Chen, C.F., Varley, N., Lavallée, Y., Kendrick, J., Reuschlé, T., 2018. Thermal resilience of microcracked andesitic dome rocks. *J. Volcanol. Geotherm. Res.* 367, 20–30.
- Heap, M.J., Kushnir, A.R., Vasseur, J., Wadsworth, F.B., Harl, P., Baud, P., Deegan, F.M., 2020. The thermal properties of porous andesite. *J. Volcanol. Geotherm. Res.* 398, 106901.
- Heap, M.J., Jessop, D.E., Wadsworth, F.B., Rosas-Carbajal, M., Komorowski, J.C., Gilg, H.A., Moretti, R., 2022. The thermal properties of hydrothermally altered andesites from La Soufrière de Guadeloupe (Eastern Caribbean). *J. Volcanol. Geotherm. Res.* 421, 107444.
- Heap, M.J., Wadsworth, F.B., Jessop, D.E., 2023. The thermal conductivity of un lithified granular volcanic materials: the influence of hydrothermal alteration and degree of water saturation. *J. Volcanol. Geotherm. Res.* 435, 107775.
- Hofmeister, A.M., 2018. *Measurements, Mechanisms, and Models of Heat Transport*. Elsevier.
- Hofmeister, A., 2020. *Heat Transport and Energetics of the Earth and Rocky Planets*. Elsevier.
- Hofmeister, A.M., Sehlke, A., Avard, G., Bollasina, A.J., Robert, G., Whittington, A.G., 2016. Transport properties of glassy and molten lavas as a function of temperature and composition. *J. Volcanol. Geotherm. Res.* 327, 330–348.
- Horai, K., Simmons, G., Kanamori, H., Wones, D., 1970. Thermal diffusivity, conductivity and thermal inertia of Apollo 11 lunar material. *Geochim. Cosmochim. Acta* 1, 2243.
- Howell, J.R., Mengüç, M.P., Daun, K.J., 2023. *Thermal Radiation: An Introduction*. CRC Press.
- Huppert, H.E., Sparks, R.S.J., 1981. The fluid dynamics of a basaltic magma chamber replenished by influx of hot, dense ultrabasic magma. *Contrib. Mineral. Petrol.* 75 (3), 279–289.
- Irvine, T.N., 1970. Heat transfer during solidification of layered intrusions. I. Sheets and sills. *Can. J. Earth Sci.* 7 (4), 1031–1061.
- Jodry, C., Heap, M.J., Bayramov, K., Alizada, G., Rustamova, S., Nabiyeva, S., 2023. Influence of high temperature on the physical and mechanical properties of porous limestone from Baku (Azerbaijan). *Fire* 6 (7), 263.
- Kant, M.A., Ammann, J., Rossi, E., Madonna, C., Höser, D., Rudolf von Rohr, P., 2017. Thermal properties of Central Aare granite for temperatures up to 500 C: irreversible changes due to thermal crack formation. *Geophys. Res. Lett.* 44 (2), 771–776.
- Kawada, K., 1964. 35. Studies of the thermal state of the Earth. The 15th paper: variation of thermal conductivity of rocks. Part I. *Bull. Earthquake Res. Inst.* 42 (4), 631–647.
- Kemmer, G., Keller, S., 2010. Nonlinear least-squares data fitting in Excel spreadsheets. *Nat. Protoc.* 5 (2), 267–281.
- Keszthelyi, L., 1994. Calculated effect of vesicles on the thermal properties of cooling basaltic lava flows. *J. Volcanol. Geotherm. Res.* 63 (3–4), 257–266.
- Klein, A., Jessop, D.E., Donnadiou, F., Moretti, R., 2024. Dome permeability and fluid circulation at La Soufrière de Guadeloupe implied from soil CO<sub>2</sub> degassing, thermal flux and self potential. *Bull. Volcanol.* 86 (4), 26.
- Lavallée, Y., Hess, K.U., Cordonnier, B., Bruce Dingwell, D., 2007. Non-Newtonian rheological law for highly crystalline dome lavas. *Geology* 35 (9), 843–846.
- Lenhardt, N., Götz, A.E., 2015. Geothermal reservoir potential of volcanoclastic settings: the Valley of Mexico, Central Mexico. *Renew. Energy* 77, 423–429.
- Liu, J., Chang, Z., Wang, L., Xu, J., Kuang, R., Wu, Z., 2020. Exploration of basalt glasses as high-temperature sensible heat storage materials. *ACS Omega* 5 (30), 19236–19246.
- Loncar, M., Huppert, H.E., 2022. Dyke cooling upon intrusion: subsequent shape change, cooling regimes and the effect of further magma input. *Earth Planet. Sci. Lett.* 593, 117687.
- Merriman, J.D., Hofmeister, A.M., Roy, D.J., Whittington, A.G., 2018. Temperature-dependent thermal transport properties of carbonate minerals and rocks. *Geosphere* 14 (4), 1961–1987.
- Merriman, J.D., Whittington, A.G., Hofmeister, A.M., 2023. A mineralogical model for thermal transport properties of rocks: verification for low-porosity, crystalline rocks at ambient conditions. *J. Petrol.* 64 (3), egad012.
- Miao, S.Q., Li, H.P., Chen, G., 2014. Temperature dependence of thermal diffusivity, specific heat capacity, and thermal conductivity for several types of rocks. *J. Therm. Anal. Calorim.* 115, 1057–1063.
- Mielke, P., Nehler, M., Bignall, G., Sass, I., 2015. Thermo-physical rock properties and the impact of advancing hydrothermal alteration—A case study from the Tauhara geothermal field, New Zealand. *J. Volcanol. Geotherm. Res.* 301, 14–28.
- Mielke, P., Weinert, S., Bignall, G., Sass, I., 2016. Thermo-physical rock properties of greywacke basement rock and intrusive lavas from the Taupo Volcanic Zone, New Zealand. *J. Volcanol. Geotherm. Res.* 324, 179–189.
- Mielke, P., Bär, K., Sass, I., 2017. Determining the relationship of thermal conductivity and compressional wave velocity of common rock types as a basis for reservoir characterization. *J. Appl. Geophys.* 140, 135–144.
- Miranda, M.M., Matos, C.R., Rodrigues, N.V., Pereira, A.J., Costa, J.J., 2019. Effect of temperature on the thermal conductivity of a granite with high heat production from Central Portugal. *J. Iber. Geol.* 45 (1), 147–161.
- Mostafa, M., Afify, N., Gaber, A., Abu Zaid, E., 2004. Investigation of thermal properties of some basalt samples in Egypt. *J. Therm. Anal. Calorim.* 75 (1), 179–188.
- Mottaghy, D., Vosteen, H.D., Schellschmidt, R., 2008. Temperature dependence of the relationship of thermal diffusivity versus thermal conductivity for crystalline rocks. *Int. J. Earth Sci.* 97, 435–442.
- Moune, S., Moretti, R., Burtin, A., Jessop, D.E., Didier, T., Robert, V., Buscetti, M., 2022. Gas monitoring of volcanic-hydrothermal plumes in a tropical environment: the case of La Soufrière de Guadeloupe unrest volcano (Lesser Antilles). *Front. Earth Sci.* 10, 795760.
- Murase, T., McBirney, A.R., 1970. Thermal conductivity of lunar and terrestrial igneous rocks in their melting range. *Science* 170 (3954), 165–167.
- Nabelek, P.L., Hofmeister, A.M., Whittington, A.G., 2012. The influence of temperature-dependent thermal diffusivity on the conductive cooling rates of plutons and temperature-time paths in contact aureoles. *Earth Planet. Sci. Lett.* 317, 157–164.
- Nahhas, T., Py, X., Sadiki, N., 2019. Experimental investigation of basalt rocks as storage material for high-temperature concentrated solar power plants. *Renew. Sust. Energy Rev.* 110, 226–235.
- Norden, B., Förster, A., Förster, H.J., Fuchs, S., 2020. Temperature and pressure corrections applied to rock thermal conductivity: impact on subsurface temperature prognosis and heat-flow determination in geothermal exploration. *Geotherm. Energy* 8 (1), 1–19.
- Norton, D., Knight, J., 1977. Transport phenomena in hydrothermal systems: cooling plutons. *Am. J. Sci.* 277, 937–981.
- Pribnow, D., Williams, C.F., Sass, J.H., Keating, R., 1996. Thermal conductivity of water-saturated rocks from the KTB pilot Hole at temperatures of 25 to 300 C. *Geophys. Res. Lett.* 23 (4), 391–394.
- Ray, L., Chopra, N., Singh, S.P., Hiloidari, S., Rao, S.E., 2023. Thermal conductivity at elevated temperature, density and geochemical signatures for the massive rhyolites of the Bundelkhand Craton, Central India. *Geophys. J. Int.* 232 (3), 1742–1755.
- Robertson, E.C., Peck, D.L., 1974. Thermal conductivity of vesicular basalt from Hawaii. *J. Geophys. Res.* 79 (32), 4875–4888.
- Romine, W.L., Whittington, A.G., Nabelek, P.L., Hofmeister, A.M., 2012. Thermal diffusivity of rhyolitic glasses and melts: effects of temperature, crystals and dissolved water. *Bull. Volcanol.* 74 (10), 2273–2287.
- Seipold, U., 1998. Temperature dependence of thermal transport properties of crystalline rocks—a general law. *Tectonophysics* 291 (1–4), 161–171.
- Shane, P., Smith, V.C., Nairn, I., 2008. Millennial timescale resolution of rhyolite magma recharge at Tarawera volcano: insights from quartz chemistry and melt inclusions. *Contrib. Mineral. Petrol.* 156, 397–411.
- Sharqawy, M.H., 2013. New correlations for seawater and pure water thermal conductivity at different temperatures and salinities. *Desalination* 313, 97–104.
- Sirdesai, N.N., Mahanta, B., Ranjith, P.G., Singh, T.N., 2019. Effects of thermal treatment on physico-morphological properties of Indian fine-grained sandstone. *Bull. Eng. Geol. Environ.* 78, 883–897.
- Toyoda, S., Goff, F., Ikeda, S., Ikeya, M., 1995. ESR dating of quartz phenocrysts in the El Cajete and Battleship Rock Members of Valles Rhyolite, Valles Caldera, New Mexico. *J. Volcanol. Geotherm. Res.* 67 (1–3), 29–40.
- Tsang, S.W., Lindsay, J.M., Coco, G., Wysocki, R., Lerner, G.A., Rader, E., Kennedy, B., 2019. The heating of substrates beneath basaltic lava flows. *Bull. Volcanol.* 81 (11), 1–14.
- Tuffen, H., Castro, J.M., 2009. The emplacement of an obsidian dyke through thin ice: Hrafninnuhryggur, Krafla Iceland. *J. Volcanol. Geotherm. Res.* 185 (4), 352–366.
- Vélez, M.I., Blessett, D., Córdoba, S., López-Sánchez, J., Raymond, J., Parra-Palacio, E., 2018. Geothermal potential assessment of the Nevado del Ruiz volcano based on

- rock thermal conductivity measurements and numerical modeling of heat transfer. *J. S. Am. Earth Sci.* 81, 153–164.
- Vosteen, H.D., Schellschmidt, R., 2003. Influence of temperature on thermal conductivity, thermal capacity and thermal diffusivity for different types of rock. *Phys. Chem. Earth Parts A/B/C* 28 (9–11), 499–509.
- Wadsworth, F.B., Vasseur, J., Llewellyn, E.W., Genareau, K., Cimarelli, C., Dingwell, D.B., 2017. Size limits for rounding of volcanic ash particles heated by lightning. *J. Geophys. Res. Solid Earth* 122 (3), 1977–1989.
- Walsh, J.B., Decker, E.R., 1966. Effect of pressure and saturating fluid on the thermal conductivity of compact rock. *J. Geophys. Res.* 71 (12), 3053–3061.
- Weydt, L.M., Ramírez-Guzmán, Á.A., Pola, A., Lepillier, B., Kummerow, J., Mandrone, G., Sass, I., 2021. Petrophysical and mechanical rock property database of the Los Humeros and Acoculco geothermal fields (Mexico). *Earth Syst. Sci. Data* 13 (2), 571–598.
- Whittington, A.G., Hofmeister, A.M., Nabelek, P.I., 2009. Temperature-dependent thermal diffusivity of the Earth's crust and implications for magmatism. *Nature* 458 (7236), 319–321.
- Wooster, M.J., Wright, R., Blake, S., Rothery, D.A., 1997. Cooling mechanisms and an approximate thermal budget for the 1991–1993 Mount Etna lava flow. *Geophys. Res. Lett.* 24 (24), 3277–3280.
- Zhao, X.G., Zhao, Z., Guo, Z., Cai, M., Li, X., Li, P.F., Wang, J., 2018. Influence of thermal treatment on the thermal conductivity of Beishan granite. *Rock Mech. Rock. Eng.* 51, 2055–2074.
- Zhou, W.X., Cheng, Y., Chen, K.Q., Xie, G., Wang, T., Zhang, G., 2020. Thermal conductivity of amorphous materials. *Adv. Funct. Mater.* 30 (8), 1903829.